ELSEVIER

Journal of Alloys and Compounds 262–263 (1997) 492–497

Journal of ALLOYS AND COMPOUNDS

Antiferromagnetic ordering in the novel Dy_3Ge_4 and $DyGe_{1.3}$ compounds studied by neutron diffraction and magnetic measurements

O. Oleksyn[a,*], P. Schobinger-Papamantellos[a], C. Ritter[b], C.H. de Groot[c], K.H.J. Buschow[c]

[a] *Laboratorium für Kristallographie, ETHZ, CH-8092 Zürich, Switzerland*
[b] *Institut Laue-Langevin, 156X, 38042 Grenoble Cédex, France*
[c] *Van der Waals-Zeeman Institute, University of Amsterdam, 1018 XE Amsterdam, The Netherlands*

Abstract

The magnetic ordering of the novel binary compounds Dy_3Ge_4 and $DyGe_{1.3(1)}$ has been studied by neutron diffraction and magnetic measurements. Dy_3Ge_4 with the Er_3Ge_4 structure type (space group *Cmcm*) displays a two step antiferromagnetic ordering below $T_N = 19$ K. The two Dy sites (Dy_1:8(f) and Dy_2:4(c)) order independently with two distinct order parameters associated with the same wave vector $q = (0, 1, 0)$. Both sublattices have a uniaxial antiferromagnetic moment arrangement but with mutually perpendicular orientations. Dy_1 orders below T_N with the moments along the *a*-axis, Dy_2 orders only below $T_t = 6$ K along the *c*-axis. At 1.4 K the moment values of Dy_1 and Dy_2 are 7.31(8) μ_B and 5.6(3) μ_B, respectively. Their arrangement leads to a symmetry reduction described by the monoclinic magnetic space group $Cp11\frac{2_1'}{m}1'(Sh_{11}^{55})$. The two-dimensional canted antiferromagnetic structure is the result of a strong magnetocrystalline anisotropy and the presence of various types of magnetic interactions. The phase of $DyGe_{1.3(1)}$ composition with the AlB_2 structure type (space group $P6/mmm$) was detected as an impurity in the studied sample. It orders antiferromagnetically below $T_N = 16$ K with collinear moment arrangement associated with a $2c$-cell enlargement ($q = 0, 0, 1/2$) described by the magnetic space group $P_{2_1}11\frac{2'}{m'}(Sh_{11}^{50})$. At 1.4 K $\mu_{Dy} = 7.2(2)$ μ_B and is confined to the (001) plane.

Keywords: Rare-earth germanides; Antiferromagnetism; Magnetic structures; Neutron diffraction

1. Introduction

Eremenko and co-workers investigated systematically [1–4] the R–Ge (R = rare-earth) binary phase diagrams. They report the formation of a novel compound of the stoichiometry R_4Ge_5 by peritectoid (Ho, Er, Lu) or peritectic (Tm) reactions.

A crystal structure determination [5] has shown the exact composition of these isomorphic phases to be R_3Ge_4 (R = Tb, Dy, Ho, Er, Tm). The structure of the orthorhombic R_3Ge_4 can be seen as a binary variant of the W_3CoB_3 structure. The structure comprises two R- and three Ge-sites. The R-atoms form trigonal prisms centred by Ge atoms and stacked along the *a* axis. Within the (0,*y*,*z*) plane adjacent prisms along *b* or *c* are shifted by x = 1/2 (see Fig. 3).

The magnetic ordering of the isomorphic R_3Ge_4 compounds is of interest as it gives a possibility to follow the influence of the *R*-component to the competing intrasite I_{AA}, I_{BB} and intersite I_{AB} interactions which may lead to complex ordering phenomena.

* Corresponding author. On leave from the Institute of Inorganic Chemistry, Lviv State University, Lviv, Ukraine.

0925-8388/97/$17.00
PII S0925-8388(97)00316-7

Recently we studied the magnetic ordering of the Er_3Ge_4 compound [6]. The two Er-sublattices order simultaneously below 7.3 K with a triangular antiferromagnetic moment arrangement within the $(0,y,z)$ plane. Adjacent prisms display different chiralities. The Er_1 magnetic moments make an angle of 35.5(3) degrees with the b-axis in the $(0,y,z)$ plane while the Er_2 moments point towards the c-axis. At 4 K a reorientation of the Er_1 moments within the $(0,y,z)$ plane sets in without any change in symmetry. At 1.5 K ordered magnetic moment values are 7.32(5) μ_B/Er_1 and 6.37(6) μ_B/Er_2, respectively.

The present paper describes the magnetic ordering of the Dy_3Ge_4 compound.

2. Sample preparation

The polycrystalline sample of composition Dy_3Ge_4 was prepared by arc melting of the elements in an atmosphere of purified argon gas. The purity of the starting materials was 99.9% for Dy and 99.99% for Ge. After arc melting the sample was vacuum annealed at a temperature of 800°C for 3 weeks and subsequently quenched in water. The purity of the sample was examined by X-ray powder diffraction. The sample contained a small amount of an additional phase.

3. Magnetic measurements

Magnetic measurements were made with a SQUID magnetometer. The temperature dependence of the reciprocal susceptibility is shown in Fig. 1a. Curie Weiss behaviour is followed down to about 17 K. From the slope and the intercept with the horizontal axis we derive the values $\mu_{eff} = 10.3$ μ_B/Dy and $\theta_p = -11$ K for the effective moment and the asymptotic Curie temperature, respectively. The former value is close to the free ion value (10.63 μ_B/Dy). In the low-field range the magnetic isotherm at 5 K (Fig. 1b) is characteristic of antiferromagnetic behaviour. There is a small break at about 3 T, indicative of a field-induced magnetic moment rearrangement. The magnetization reached in the highest field applied corresponds to 6.1 μ_B/Dy.

4. Neutron diffraction

Neutron diffraction experiments were carried out at the facilities of the ILL reactor (Grenoble) D1B diffractometer ($\lambda = 2.52$ Å). To counterbalance the high absorption cross-section of Dy for neutrons the sample was diluted with Al powder (ratio 1:1) and filled up into a sample holder of 5-mm diameter. The data were collected in the temperature range 1.4–23 K with an increment in T of 0.5 K. The step increment in 2θ was 0.2°. The data analysis was performed by the Fullprof program [7] with pseudo-Voight function used for the peak shape fit.

4.1. Crystal structure of Dy_3Ge_4

The 20 K refined neutron pattern in the paramagnetic state confirms the structure and atomic parameters reported in [5] (Fig. 2 (top part) and Table 1). The refinement comprises the Al-powder pattern as well as the coexisting $DyGe_{1.3}$ phase of the AlB_2 type (Sec. 4.5).

4.2. The magnetic ordering of Dy_3Ge_4 in the range T_N–T_i

At temperatures below $T_N = 19$ K magnetic order sets in. All observed magnetic lines (i.e. the strong (011) line in the low 2θ region in Fig. 2 (bottom part)) do not obey the C-lattice reflection condition. The wave vector is $q = (0,1,0)$ which corresponds to the anticentered magnetic C_P lattice. There are eight magnetic space groups associated with the *Cmcm* space group and the wave vector $q = (0,1,0)$ [8].

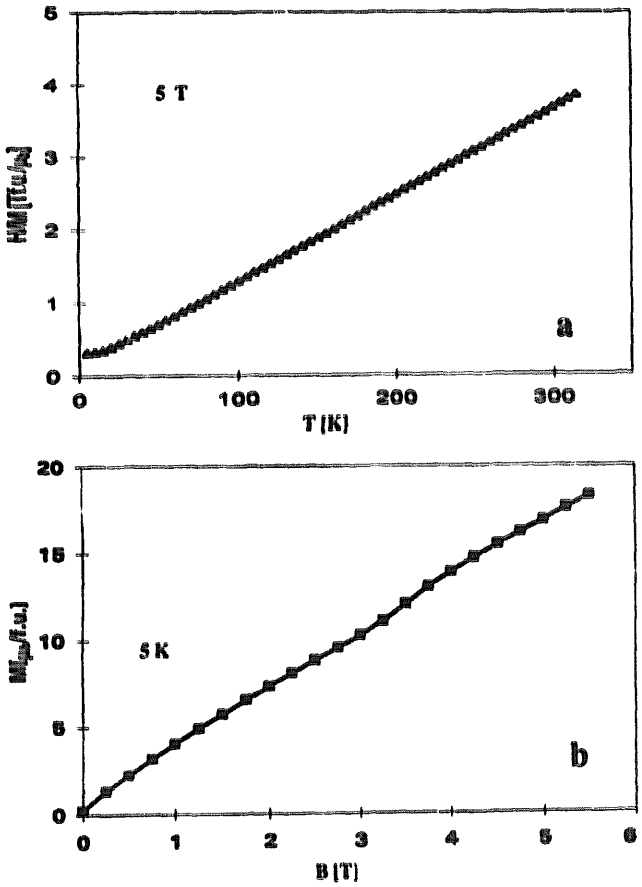

Fig. 1. Temperature dependence of the reciprocal susceptibility of Dy_3Ge_4 plotted from magnetisation data obtained under a field of 5 T (a). Field dependence of the magnetic moment measured at 5 K (b).

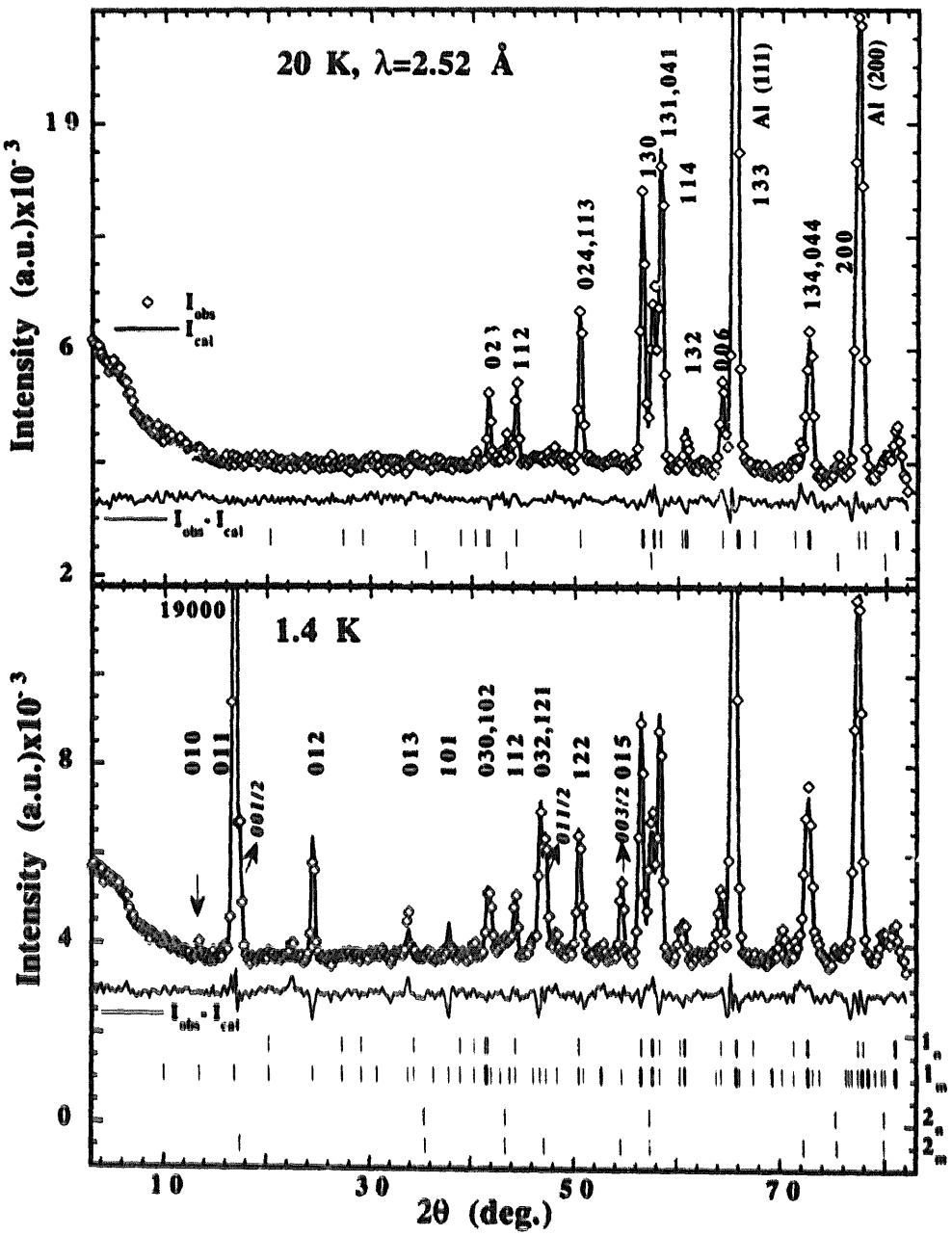

Fig. 2. Observed, calculated and difference neutron diagram of a two-phase sample measured (a) in the paramagnetic state at 20 K (top part), (b) in the magnetically ordered state at 1.4 K (bottom part). Four reflection sets labelled by 1_n, 1_m, 2_n, 2_m in the right margin correspond to nuclear and magnetic contributions of Dy_3Ge_4 and $DyGe_{1.911}$, respectively. Main magnetic contributions of Dy_3Ge_4 are indexed in bold and $DyGe_{1.911}$ in italic letters.

The possible magnetic modes of the 8(f) and 4(c) Wyckoff positions occupied by the Dy atoms are as displayed in Table 2 in Ref. [6]. The 8(f) site may have also a two-dimensional ordering. The 4(c) site may have only a uniaxial type of ordering with either an A(+ − − +) or a C(+ + − −) mode. The refinement of the magnetic intensities indicates that over the entire T_N–T_t interval only the 8(f) site is ordering with a collinear arrangement of the Dy_1 magnetic moments directed along the *a*-axis. The atoms (1) $(0,y,z)$ and (2) $(0,-y,1/2+z)$ related by the 2_{1z} operation have the same signs while the atoms (1) and (3) $(0,y,1/2-z)$ related by the 2_y operation have the opposite signs. Taking into consideration the C_P anti-translation one obtains the mode C_x-C_x (+ + − − − − + +) in the notation of [8]. This arrangement remains invariant under the transformations of the magnetic space group $Cp\frac{2'2'2_1'}{mc'm}i'(Sh_{59}^{414})$.

4.3. Magnetic structure of Dy_3Ge_4 at 1.4 K

At temperatures below $T_t = 6$ K the relative intensities of the magnetic reflections are modified. As the

Table 1
Refined parameters from neutron data of Dy_3Ge_4 (space group *Cmcm*) and $DyGe_{1.3(1)}$ (space group *P6/mmm*): (a) at 20 K (paramagnetic state) (b) at 1.4 K in the magnetically ordered state (magnetic space groups $Cp11\frac{2_1'}{m}i'(Sh_{11}^{55})$ and $P_{2c}11\frac{2'}{m'}(Sh_{11}^{56})$, respectively)

Dy_3Ge_4 Atom	20 K		1.4 K	
	y	*z*	*y*	*z*
Dy_1 at 8f: (0,*y*,*z*)	0.335(1)	0.099(1)	0.3336(9)	0.0987(9)
Dy_2 at 4c: (0,*y*,1/4)	0.055(2)	0.25	0.055(2)	0.25
Ge_1 8f: (0,*y*,*z*)	0.357(5)	0.8880(6)	0.353(5)	0.888(2)
Ge_2 at 4c: (0,*y*,1/4)	0.784(5)	0.25	0.789(6)	0.25
Ge_3 at 4a: (0,0,0)	0.0	0.0	0.0	0.0
μ_{xDy1}, μ_{zDy2} [μ_B]			7.36(8)	−5.7(3)
a, *b*, *c* [Å]	4.027(1), 10.599(3), 14.169(5)		4.0242(9), 10.602(3), 14.175(4)	
R_n%, R_m%	6.8, —		4.9, 8.4	
R_{wp}%, R_{exp}%	9.7, 6.2		10.9, 5.4	
$DyGe_{1.3(1)}$	20 K		1.4 K	
Atom	occup.		μ_x [μ_B]	
Dy at 1a: (0,0,0)	1		7.2(2)	
Ge at 2d: (1/3,2/3,1/2)	0.63(8)			
a, *c* [Å]	3.920(2)	4.119(4)	3.918(2)	4.1191(7)
R_n%, R_m%	9.5, —		8.3, 6.2	

structure has two inequivalent *R*-sites we assumed that the observed changes are associated with the ordering of Dy_2 moments and/or with a possible reorientation of Dy_1 moments away from the *x*-direction.

The refinement has converged ($R_n = 4.9\%$, $R_m = 8.4\%$, $R_{wp} = 10.9\%$, $R_{exp} = 5.4\%$, Table 1 and Fig. 2) for a collinear arrangement of the Dy_2 magnetic moments along the *c*-axis and Dy_1 — along the *a*-axis. The Dy_2 atoms (1) (0,*y*,1/4) and (2) (0,−*y*,3/4) related by the *i* operation have opposite signs. Implying the C_p antitranslation operation one obtains the A(+ − − +) mode. The ordering of the Dy_2 sublattice is described by the magnetic space group $Cp\frac{22'2_1'}{m'cm}i'(Sh_{57}^{391})$. The magnetic space group common for the Dy_1 and Dy_2 sublattices has only monoclinic symmetry $Cp11\frac{2_1}{m}i'(Sh_{11}^{55})$. The ordered moment values of the Dy_1 and Dy_2 sites are 7.36(8) and 5.7(3) μ_B/Dy, respectively. These values are lower than the free-ion value of Dy^{3+} ($gJ[\mu_B] = 10[\mu_B]$).

As already mentioned in Sec. 1 the structure consists of trigonal prisms formed by the Dy-atoms centered by the Ge_2-site which form infinite slabs along the *a*-period. Prisms related by the C-centering have the same alignment while prisms related by the center of symmetry are magnetically inverted (Fig. 3a). Within the Dy_1 and Dy_2 [100] chains (Dy-Dy distance equal to $a = 4.0240(9)$ Å), the interaction is ferromagnetic. This facilitates the description of the magnetic structure as it is sufficient first to describe the coupling within the isosceles triangular prism base formed by $2Dy_1$ and $1Dy_2$ atoms in the (0,*y*,*z*) plane. The mutual orientation of the four prisms (triangles) in the cell is then given by applying the C_p and *i'* symmetry operations.

In each triangle the coupling between two adjacent Dy_1 moments (next neighbours at a distance of 4.28(2) Å) is antiferromagnetic and the moments point perpendicularly to the plane of the triangle. The third atom in the triangle, Dy_2, is located at the nearest neighbour distance $Dy_2 - Dy_1$ equal to 3.65(2) Å, its moment points towards the *z*-direction. This arrangement is ferrimagnetic and differs from that encountered in Er_3Ge_4 (planar antiferromagnetic triangular arrangement with zero net moment).

4.4. Thermal evolution of magnetic order in Dy_3Ge_4

Fig. 4 (top part) shows the thermal evolution of integrated intensities extracted by a Gaussian fit of selected magnetic peaks. The intensity of the weak (102) reflection displays a smooth increase with decreasing temperature while the intensity of the (011) reflection shows a discontinuity and a slope change at $T_t = 6$ K. The magnetic structure factor of the (102) reflection has only contributions arising from the μ_{xDy1} component while the structure factor of the (011) reflection comprises contributions of both μ_{xDy1} and μ_{zDy2} moments which add up: $F(011) \sim 4 \times (1.428\mu_{xDy1} + 0.945\mu_{zDy2})$.

The thermal behaviour of the magnetic intensities suggests a two-step magnetic ordering of the two sublattices. Below T_N the Dy_1 moment increases smoothly with decreasing temperature (see Fig. 4, bottom part). The ordered Dy_2 moment evolves only

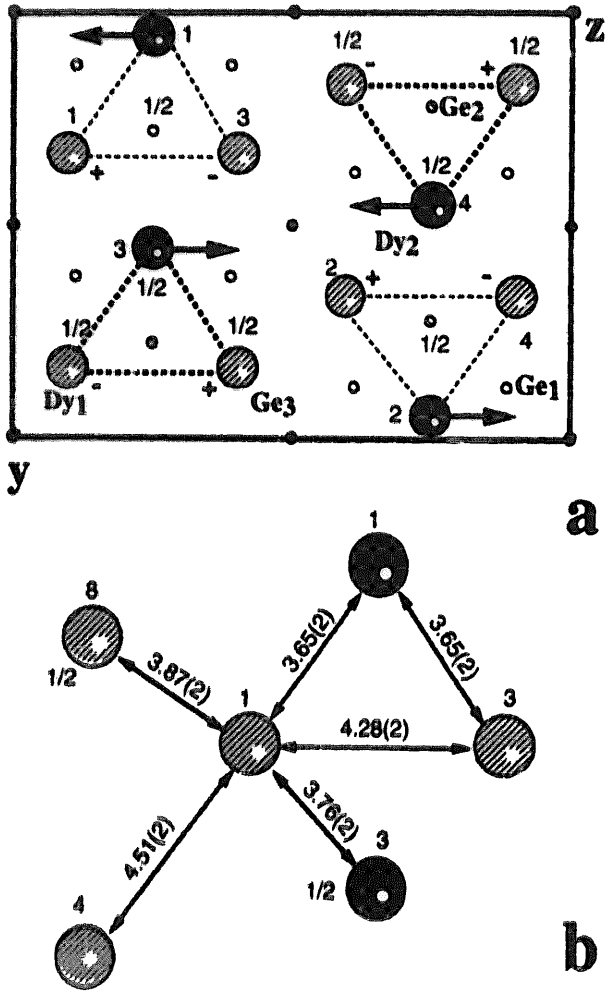

Fig. 3. Canted moment arrangement of Dy_3Ge_4 when viewed along the [100] direction (a). Shortest interatomic Dy-Dy distances (b).

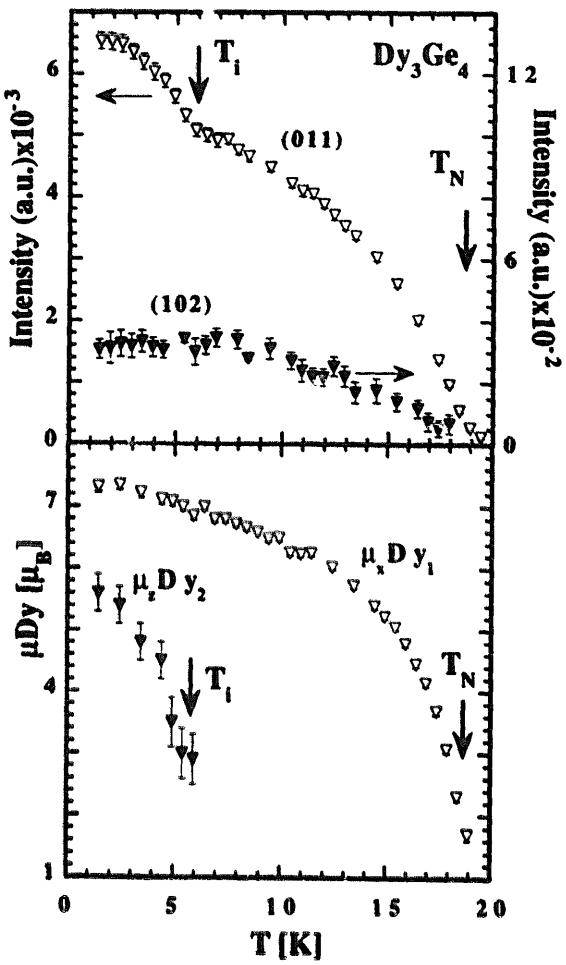

Fig. 4. Thermal variation of the (011) and (102) magnetic intensities (top part) and of the magnetic moments in Dy_3Ge_4.

below $T_1 = 6$ K. The slope of the μ_{zDy2} vs. T curve is steeper than that of μ_{xDy1} vs. T as the Dy_1 moment has already achieved its saturation value around T_1.

4.5. Crystal and magnetic structures of $DyGe_{1.3(1)}$

The 20 K neutron data comprise next to the nuclear reflections of the Dy_3Ge_4 phase additional reflections of a secondary phase. These lines were indexed in the AlB_2 structure type (space group *P6/mmm*). In agreement with [9] we found that the AlB_2 structure is realised at a non-stoichiometric composition. The simultaneous refinement of Dy_3Ge_4 and $DyGe_{1.3(1)}$ parameters (Table 1, Fig. 2) shows that the amount of the latter does not exceed 5%. The refined composition of the $DyGe_{1.3(1)}$ is very close to the composition of the major phase ($DyGe_{1.33}$). This fact in addition to the peritectoid way of formation of Dy_3Ge_4 explains the difficulties in synthesis of a single phase sample.

In the 1.4 K neutron data additional lines of magnetic origin were observed and indexed with a $2c$-cell enlargement ($q = 001/2$) of the $DyGe_{1.3(1)}$ chemical unit cell. From the presence of the dominating (001/2) reflection it can be inferred that the magnetic moments are confined to the (001) plane. The refinement leads to a collinear antiferromagnetic arrangement of the Dy moments perpendicular to the hexagonal axis. This arrangement remains invariant under the transformations of the magnetic space group $P_{2c}11\frac{2'}{m'}(Sh_{11}^{66})$. At 1.4 K the ordered moment value is $\mu_{Dy} = 7.2(2)\ \mu_B$/atom. The thermal behaviour of the (001/2) reflection reveals the ordering temperature of $T_N = 16$ K (Fig. 5). Due to the small amount of $DyGe_{1.3(1)}$ in the studied sample additional information is needed to verify these results.

5. Conclusions

The magnetic structures and phase transitions of the novel phases Dy_3Ge_4 and $DyGe_{1.3(1)}$ were studied in the 23–1.4 K interval by neutron diffraction and magnetic measurements.

A two-step magnetic ordering was found for Dy_3Ge_4. In a first step Dy_1 orders below T_N with the

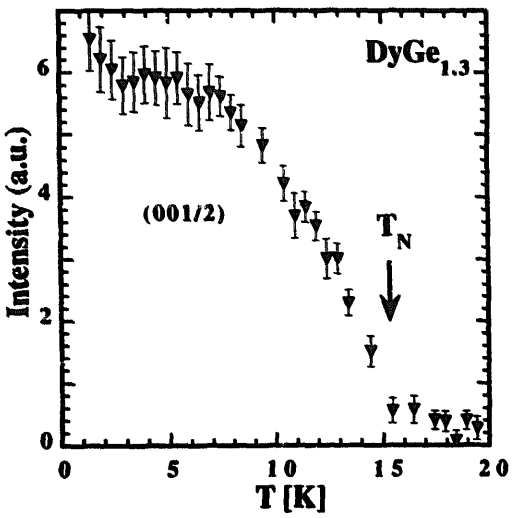

Fig. 5. Thermal variation of the (001/2) magnetic intensity of $DyGe_{1.3(1)}$.

moments aligned along the *a*-axis. The Dy_2 moments order only below $T_i = 6$ K perpendicular to Dy_1 along the *c*-axis. The two crystallographically distinct magnetic Dy sites form a two-dimensional canted antiferromagnetic structure. Each sublattice has a uniaxial antiferromagnetic moment arrangement but different preferred orientations and different ordering temperatures reflecting the presence of two distinct order parameters. This behaviour is caused by the triangular arrangement of the two sublattices within the $(0,y,z)$ plane. A number of complex ordering types due to a geometric frustration is known for triangular lattices [10].

The great variety of magnetic structures of pure heavy rare earths and their compounds can be understood as the consequence of the dominant role of the exchange interactions with the crystal field and magnetoelastic effects acting as perturbations [11]. From the evolution of magnetic order in the Dy_3Ge_4 compound it follows that the intrasublattice interaction I_{11} is the important one and it dominates in the T_N–T_i region. In each $2Dy_1$–Dy_2 triangle (see Fig. 3) the coupling between Dy_1–Dy_1 next neighbour atoms is antiferromagnetic and the moment is perpendicular to the $(0,y,z)$ plane. This creates a geometrical frustration for the ordering of the third moment Dy_2 — the latter cannot order in alignment with any of the Dy_1 moments. Only at low temperatures the interaction I_{22} becomes important and the Dy_2-sublattice orders perpendicularly to Dy_1. As the two sublattices order at different temperatures and with different ordering parameters the intersite I_{12} interaction is a rather weak one.

The observed magnetic behaviour infers that the crystal-field effects are significant in Dy_3Ge_4: they hinder the magnetic moments to attain the free Dy^{3+} ion saturation value $gJ\mu_B$ (especially of Dy_2) and fix the moments to favored directions.

The moment arrangement in Dy_3Ge_4 is different from the planar magnetic triangular antiferromagnetic arrangement (with zero net moment) encountered in Er_3Ge_4. In the latter compound magnetic ordering is described by the same order parameter for both sublattices.

The $DyGe_{1.3(1)}$ phase crystallises in the hexagonal AlB_2 structure type. The moment arrangement leads to ferromagnetic hexagonal layers coupled antiferromagnetically along the *c*-axis similar to the isomorphic silicide $TbSi_{1.67-\delta}$ [12].

Acknowledgements

This work is financially supported by the Swiss National Foundation, Bern.

References

[1] V.N. Eremenko, I.M. Obushenko, Yu.I. Buyanov, Dop. Akad. Nauk UkrRSR., Ser. A 7 (1980) 87.
[2] V.N. Eremenko, I.M. Obushenko, Izv. Vyssh. Uchebn. Zaved., Tsvet. Met. 3 (1981) 59.
[3] V.N. Eremenko, K.A. Meleshevich, Yu.I. Buyanov, V.M. Petjuch, Dop. Akad. Nauk UkrRSR., Ser. A 5 (1987) 78.
[4] V.N. Eremenko, K.A. Meleshevich, Yu.I. Buyanov, P.S. Martsenyuk, Poroshk. Met. 27 (1989) 543.
[5] O.Ya. Oleksyn, O.I. Bodak, J. Alloys Comp. 210 (1994) 19.
[6] P. Schobinger-Papamantellos, O. Oleksyn, C. Ritter, C.H. de Groot, K.H.J. Buschow, J. Magn. Magn. Mater. 169 (1997) 253.
[7] J. Rodríguez-Carvajal, Physica B 192 (1993) 55.
[8] E.F. Bertaut, in: (a) G.T. Rado, H. Suhl (Eds.), Magnetism, vol. III, Ch. 4, Academic Press, New York, 1963, p. 149. (b) Ann. Phys. 9 (1975) 93.
[9] E.I. Gladyshevskii, Zhurnal Strukturnoi Khimii 5 (1964) 523.
[10] M.W. Long, Int. J. Mod. Phys. B 7 (1993) 2981.
[11] J. Jensen, A.R. Mackintosh, Rare Earth Magnetism, Clarendon Press, Oxford, 1991.
[12] P. Schobinger-Papamantellos, D.B. de Mooij, K.H.J. Buschow, J. Magn. Magn. Mater. 79 (1989) 231.